NACA

RESEARCH MEMORANDUM

RELATION OF TURBINE-ENGINE COMBUSTION EFFICIENCY TO SECOND-ORDER REACTION KINETICS AND FUNDAMENTAL FLAME SPEED

By J. Howard Childs and Charles C. Graves

Lewis Flight Propulsion Laboratory
Cleveland, Ohio

NATIONAL ADVISORY COMMITTEE
FOR AERONAUTICS

WASHINGTON
August 24, 1954

DECLASSIFIED FEB. 10, 1956

NATIONAL ADVISORY COMMITTEE FOR AERONAUTICS

RESEARCH MEMORANDUM

RELATION OF TURBINE-ENGINE COMBUSTION EFFICIENCY TO SECOND-ORDER REACTION KINETICS AND FUNDAMENTAL FLAME SPEED

By J. Howard Childs and Charles C. Graves

SUMMARY

Previous theoretical studies of the turbojet combustion process are summarized and the resulting equations are applied to experimental data obtained from previous combustor tests. The theoretical treatment assumes that one step in the over-all chain of processes which constitute turbojet combustion is sufficiently slow to be the rate-controlling step that determines combustion efficiency. The parameter $\frac{P_i T_i}{V_r}$ (P_i is combustor-inlet static pressure, T_i is combustor-inlet static temperature, and V_r is combustor reference velocity based on P_i, T_i, and maximum combustor cross-sectional area.), based on the assumption that chemical reaction kinetics control combustion efficiency and the parameter $\frac{P_i^{1/3} T_i^{1.1}}{V_r}$, derived from the assumption that the rate of flame spreading controls combustion efficiency, are evaluated for two turbojet combustors. (In an earlier paper, $\frac{P_i T_i}{V_r}$ has been evaluated for 14 turbojet combustors.) The parameter $\frac{P_i T_i}{V_r}$ provided an adequate correlation of the combustion efficiency of one combustor at simulated engine operating conditions. The data for this combustor were not correlated by $\frac{P_i^{1/3} T_i^{1.1}}{V_r}$. Data obtained with the other combustor indicate that a shift from one rate-controlling step to another occurs as combustor pressure is increased, and the parameter $\frac{P_i T_i}{V_r}$ therefore best correlates the data at low pressures, while the

parameter $\frac{P_i^{1/3} T_i^{1.1}}{V_r}$ is better at higher pressures. No single correlating parameter can therefore be expected to be adequate for all combustors and for the entire range of operating conditions.

INTRODUCTION

One of the most serious problems encountered in the operation of jet-propelled aircraft is the reduction in combustion efficiency that occurs at high-altitude flight conditions. Experimental investigations with both turbojet and ram-jet combustors have shown that combustion efficiency is adversely affected by the high velocities at which these combustors are required to operate and by the low pressures and low inlet temperatures encountered at high altitudes. A theory of the jet-engine combustion process is therefore needed in order to explain these effects and to indicate the design approaches that are most promising for alleviating these adverse effects. This paper describes the theoretical treatment that has been given the combustion process as it occurs in turbojet combustors. Various parts of this work have been previously published (refs. 1 to 3); this report presents a brief summary of this previous work together with new data which amplify the conclusions of references 1 to 3. Similar studies have been made of the ram-jet combustion process (refs. 4 and 5); however, the analysis for ram-jet combustion differs in some details and is therefore not included herein.

If the fuel were properly mixed with air and the fuel-air mixture were allowed adequate time in the combustor, thermodynamic equilibrium would be achieved and the combustion efficiency would be 100 percent (ref. 6). The occurrence of combustion efficiencies below 100 percent indicates that the conversion processes by which the chemical energy of the fuel is converted into sensible enthalpy of the exhaust products are not rapid enough to proceed to completion during the residence time allowed in high-velocity combustors. A theoretical treatment of turbine-engine combustion is difficult because of the many different conversion processes which must occur. The fuel must be vaporized, mixed with air, ignited, and oxidized to the final products of combustion. These combustion products must then be mixed with dilution air to reduce the temperatures to values that can be tolerated by the turbine blades. The combustion can be visualized as a competition between the conversion processes (vaporization, mixing, ignition, and oxidation) and the quenching that occurs when the reacting mixture is cooled by the dilution air and when the reacting mixture comes in contact with the relatively cool walls of the combustor liner. Because of the complicated nature of the over-all process, no exact theoretical treatment is currently possible.

By making simplifying assumptions regarding the turbojet combustion process, it is possible, however, to apply theoretical considerations in the analysis of the process. If the rate of any one of the conversion processes is substantially less than the rates of the others, this one process will then govern the over-all rate and hence will determine the combustion efficiency. The existence of a single, slow conversion step in the over-all chain of processes was assumed. Theoretical treatment of the turbine engine combustion process was then made, assuming each of the various conversion steps to be the over-all rate-determining process. This paper describes the details of the analysis and demonstrates the application of the results of the analysis to experimental data obtained with two turbojet combustors.

ANALYSIS

Chemical Reaction Kinetics

One theoretical analysis of the turbojet combustion process is based on the assumption that the chemical reaction (oxidation of the fuel) constitutes the over-all rate-determining step in the combustor. This oxidation occurs by some chain mechanism. It is sometimes true, however, that the kinetics of chain reactions are dependent entirely upon the kinetics of a single, slowly occurring reaction within the chain. The analysis described herein was therefore based on the kinetics of a bimolecular chemical reaction (ref. 1).

For the bimolecular reaction

$$A + B \rightarrow C + D$$

in which A is the reactant present in smaller quantity, the reaction rate is given by the equation

$$\frac{dw}{d\theta} = \frac{Z\varphi_B}{N_A} \tag{1}$$

(All symbols are defined in the appendix.) Substituting appropriate relations from the kinetic theory of gases (ref. 7) leads to

$$\frac{dX}{d\theta} = \frac{1}{\rho}\frac{dw}{d\theta} = \frac{K_1 (\sigma_A + \sigma_B)^2 N_B (1 - X)\left(1 - \frac{N_A}{N_B} X\right) Pe^{-E/RT}}{R^{1/2} T^{1/2}} \tag{2}$$

Equation (2) applies to any sample of the reacting mixture as it passes through the combustor.

At this point in the analysis, two somewhat different approaches are taken. These are treated as the nonhomogeneous reactor and the homogeneous reactor, respectively.

Nonhomogeneous reactor. - Figures 1 and 2 show values of fuel-air mixture composition within the burning zone of a typical turbojet combustor; these data were obtained by a water-cooled sampling probe. The vapor fuel-air ratio decreases progressively along the length of the combustor, and marked variations in composition occur over the combustor cross section. The data of figures 1 and 2 indicate that homogeneity is not approached. The rate of mixing of fuel and air may nevertheless be quite rapid. The assumption of rapid fuel-air mixing is made in this portion of the paper; possible effects of slow mixing rates will be subsequently treated under Other Processes.

The major assumptions contained in this analysis may be summarized as follows:

(1) Reaction occurs in local stoichiometric fuel-air-ratio zones which exist at the interface between the fuel-rich and air-rich regions.

(2) The mixing process whereby fuel and air are introduced to the reaction zone is sufficiently rapid so that the chemical reaction rate controls the over-all process.

(3) The temperature in the reaction zone is constant along the combustor at a value close to the stoichiometric flame temperature.

(4) The mean concentration of each reactant in the reaction zone varies along the combustor and is equal to the initial concentration minus the fraction X that has already reacted at any position in the combustor.

The foregoing assumptions do not necessarily constitute those characterizing the simplest or most plausible physical model of the combustion process. Rather, they constitute the assumptions necessary to arrive at a final equation which fits the experimental data.

At the outlet of the reaction zone, X is equal to η_b because the particular reaction under consideration is the one governing the over-all process. Thus,

$$X = \eta_b \quad \text{when} \quad l = L \quad \text{and} \quad \theta = L/V_a \tag{3}$$

Integrating equation (2) with the assumption that the temperature in the zone where the reaction

$$A + B \rightarrow C + D$$

occurs is substantially constant, and substituting from equation (3),

$$\ln \frac{1 - \frac{N_A}{N_B}\eta_b}{1 - \eta_b} + K_2 = \frac{K_1 (\sigma_A + \sigma_B)^2 (N_B - N_A) L P e^{-E/RT}}{V_a R^{1/2} T^{1/2}} \tag{4}$$

The foregoing equation is expressed in terms of the values of P, T, and V_a in the reaction zone. In experimental investigations, these variables are not measured; the values of the combustor-inlet variables P_i, T_i, and V_r are usually determined, however. The values of P, T, and V_a must therefore be expressed in terms of combustor-inlet conditions; when appropriate approximations and substitutions are made,

$$\ln \frac{1 - \frac{N_A}{N_B}\eta_b}{1 - \eta_b} + K_2 = \left[K_1 \frac{(\sigma_A + \sigma_B)^2 (N_B - N_A) e^{-E/RT}}{R^{1/2} T^{3/2}} \right] \left[\frac{L \left(1 - \frac{\Delta P}{P_i} \right)^2}{\left(\frac{A_{H,P}}{A_{H,T}} \right) \left(\frac{A_r}{A_a} \right)} \right] \left(\frac{P_i T_i}{V_r} \right) \tag{5}$$

On the right side of equation (5) the terms are grouped into (1) those dependent upon fuel type and fuel-air ratio, (2) those dependent upon combustor design, and (3) those dependent only upon the operating conditions.

For a given combustor operating with a given fuel at a fixed fuel-air ratio and assuming negligible pressure drop across the combustor, equation (5) becomes

$$\ln \frac{1 - \frac{N_A}{N_B}\eta_b}{1 - \eta_b} + K_2 = K_3 \frac{P_i T_i}{V_r} \tag{6}$$

The same relation can be expressed as

$$\eta_b = f\left(\frac{P_i T_i}{V_r} \right) \tag{7}$$

Figures 3 and 4 show experimental data obtained with turbojet combustor A plotted in accordance with equations (6) and (7), respectively. A straight-line data correlation is obtained in figure 3, as predicted by equation (6). Data for a range of fuel-air ratios are included in both figures 3 and 4. The theoretical equations apply only for a fixed

fuel-air ratio; however, it was noted that for this particular combustor, the efficiency did not vary appreciably with change in fuel-air ratio in the range investigated.

Reference 1 presents a detailed derivation of equations (6) and (7) and discusses the application of equation (7) to data obtained with 14 turbojet combustors. For some combustors, the correlation is good, but for others, the data scatter is great and the parameter $\frac{P_i T_i}{V_r}$ cannot be used to predict combustion efficiency. Equation (7) has nevertheless been widely used to correlate combustion-efficiency data obtained at the NACA Lewis laboratory in single combustor tests (for example, ref. 1) and in full-scale engine tests (for example, ref. 8). Reference 8 presents data for a combustor in which combustion efficiency varies appreciably with fuel-air ratio; for this combustor, a satisfactory correlation was obtained by using a different correlation curve for each narrow range of fuel-air ratio.

Homogeneous reactor. - With the assumption that the mixing in the combustor is sufficiently rapid to produce a homogeneous mixture throughout the combustor volume, for given operating conditions the value of X is constant over the combustor reaction zone, and it is no longer necessary to integrate the equation as was done in the preceding analytical approach. The assumption of a homogeneous reactor was also made in reference 9 in analyzing the combustion process in a can-type combustor having a premixed fuel-air feed and in reference 10 in analyzing flames in the wake of bluff bodies.

For this condition $T = T_i + K_4 \Delta T_s \eta_b$,

$$\eta_b \equiv \left(\frac{dw}{d\theta}\right)\left(\frac{1}{\rho}\right)\theta = \frac{K_1 (\sigma_A + \sigma_B)^2 N_B (1 - \eta_b)\left(1 - \frac{N_A}{N_B}\eta_b\right) PLe^{-E/R(T_i + K_4 \Delta T_s \eta_b)}}{R^{1/2} (T_i + K_4 \Delta T_s \eta_b)^{1/2} V_a} \tag{8}$$

Rearranging terms yields

$$\frac{\eta_b (T_i + K_4 \Delta T_s \eta_b)^{3/2} e^{\frac{E}{R(T_i + K_4 \Delta T_s \eta_b)}}}{(1 - \eta_b)\left(1 - \frac{N_A}{N_B}\eta_b\right)} = \left[\frac{K_1 (\sigma_A + \sigma_B)^2 N_B}{R^{1/2}}\right]\left[\frac{L\left(1 - \frac{\Delta P}{P_i}\right)^2}{\left(\frac{A_{H,P}}{A_{H,t}}\right)\left(\frac{A_r}{A_a}\right)}\right]\left(\frac{P_i T_i}{V_r}\right) \tag{9}$$

Here again the terms on the right side of the equation are grouped into (1) those dependent upon fuel type and fuel-air ratio, (2) those dependent upon combustor design, and (3) those dependent only upon operating conditions. For a given combustor, a given fuel, and a single fuel-air ratio, equation (9) becomes

$$\frac{\eta_b \left(T_i + K_4 \Delta T_s \eta_b\right)^{3/2} e^{\frac{E}{R(T_i + K_4 \Delta T_s \eta_b)}}}{(1 - \eta_b)\left(1 - \frac{N_A}{N_B} \eta_b\right)} = K_3 \frac{P_i T_i}{V_r} \tag{10}$$

The data for combustor A were plotted in accordance with equation (10). The predicted straight-line relation was not obtained, thereby indicating that the assumption of nonhomogeneity (eq. (6)) better fits the experimental data than does the assumption of homogeneity (eq. (10)) for this particular combustor. This is in accord with expectations, since figures 1 and 2 indicate that a condition of homogeneity is not approached within a typical turbojet combustor. For combustors having higher rates of mixing in the combustion space, equation (10) may afford a better correlation of the data. Equation (10) can also be expressed as

$$\eta_b = f\left(\frac{P_i T_i}{V_r}, T_i\right) \tag{11}$$

and since T_i is small compared with $K_4 \Delta T_s$, for a reasonable correlation of engineering data for which T_i does not vary widely, it might be assumed

$$\eta_b = f\left(\frac{P_i T_i}{V_r}\right) \tag{7}$$

This is the same equation as that obtained for the nonhomogeneous reactor.

Flame Spreading

Since flame speed is one of the fundamental combustion properties that can readily fit into a physical picture of the combustion process, a simplified analysis was also made, assuming combustion efficiency to be controlled by the rate of flame spreading. The combustion process was visualized as the burning of fuel-air mixture zones of random size and shape, which are surrounded by a flame surface and which are consumed as they pass through the combustor. The flame surface advances into the

adjacent unburned mixture at a rate determined by the physical conditions of the unburned mixture. The effect of turbulence on the rate of flame spreading is considered solely in terms of its effect on the flame surface area. This picture of the combustion process was suggested by the analysis of reference 11 in which the concept of reaction interface extension was introduced in a study of the combined effects of diffusion and chemical reaction in gaseous fuel combustion.

The combustion efficiency can be expressed approximately by the relation

$$\eta_b = \left(\frac{1}{f}\right)\left(\frac{u_f}{V_r}\right)\left(\frac{A_f}{A_r}\right) \tag{12}$$

The numerator of this expression is proportional to the rate of consumption of fuel-air mixture in the flame, and the denominator is proportional to the rate of flow of combustible mixture through the combustor. A detailed derivation of equations (12) through (17) appears in reference 2. Equation (12) is based on the assumptions of low pressure drop across the combustor and a temperature in the unburned mixture equal to the combustor-inlet temperature. The total flame surface A_f corresponds to the reaction interface extension that is treated in detail by reference 11. The value A_f represents an integration of the flame surface area per unit volume a_f over the total combustor volume.

The principal changes in a_f would appear to be associated with (1) the changes in turbulence accompanying the energy release per unit mass of air along the combustor, (2) the reduction in flame area resulting from consumption of the combustible mixture, and (3) the effect of combustor-inlet variables on flame area. For a given fuel and over-all fuel-air ratio, the energy release per unit mass of air is proportional to the combustion efficiency, while the fractional volume occupied by the unburned mixture is a function of both the combustion efficiency and the inlet temperature. The effect of combustor-inlet variables on the flame surface area is treated similarly to the reaction zone interface extension of reference 11. The value a_f is a measure of the average hydraulic radius of the unburned mixture zones, or the average distance through which the flame must travel to complete the combustion process. The product of a_f, with its dimensions of reciprocal length, and a characteristic length of the combustor has a physical significance similar to that of the Nusselt number for heat transfer. As suggested by reference 11, a_f would probably be related to inlet conditions in terms of the Reynolds number. Increase in density of the unburned mixture alone will increase the flame surface area "packed" in a unit volume of the combustor, since the surface-volume ratio of any individual zone within the unit volume increases with density. As was also shown by reference 11, a_f would be proportional to

the cube root of the density. If the effects of inlet-flow variables and the actual burning process on a_f can be treated as separate functions, the total flame area A_f could be expected to be related to combustor-inlet conditions and combustion efficiency by

$$A_f = K_5 \left[(Re)^p \left(\frac{P_i}{T_i} \right)^{1/3} \right] \left[f\ (\eta_b,\ T_i) \right] \tag{13}$$

Here the terms in the first set of brackets account for the effect of combustor-inlet variables on flame area, while the term in the second brackets accounts for the effect of energy release and reduction in volume of unburned mixture on flame area. Substituting equation (13) in equation (12) and neglecting the probable small effect of inlet temperature on the fractional volume occupied by unburned mixture yields

$$\eta_b = f \left[K_6 \left(\frac{P_i}{T_i} \right)^{1/3} \left(\frac{u_f}{V_r} \right) Re^p \right] \tag{14}$$

Here K_6 is a constant for a given combustor, fuel, and over-all fuel-air ratio.

The use of equation (14) for normal combustor operating data requires knowledge of the effect of ambient temperature and pressure on laminar flame speed and the effect of Reynolds number on turbulent flame speed. In reference 12, the laminar flame speeds of vapor isooctane-oxygen-nitrogen mixtures at atmospheric pressure and various equivalence ratios were determined over a range of initial mixture temperatures and oxygen concentrations. The maximum flame speed was found to be proportional to the 1.4 power of the initial mixture temperature. This temperature dependency was assumed to be representative for the fuel used in combustor A.

The effect of variations in ambient pressure on the laminar flame speeds of hydrocarbon fuel-air mixtures has not been definitely established. The effect, if any, is small and appears to vary with fuel type. In general, the relation between the flame speed and pressure can be expressed in the form

$$u_f = K_7\ P_i^{\ q} \tag{15}$$

for hydrocarbon fuel-air mixtures. Here q generally has a value ranging from -1/3 to approximately 0. In reference 13 it is concluded that the flame speeds of hydrocarbon fuel-air mixtures should be independent of pressure provided that the tube diameter is large enough to prevent surface effects from becoming important. In reference 14, the flame speed

of vaporized isooctane-air mixtures was found to be inversely proportional to the cube root of the ambient pressure. Reference 15 shows the exponent q in equation (15) to be dependent on the flame speed of the fuel. For fuels having flame speeds of the order of that of isooctane, the value of q is zero. In view of the conflicting data available in the literature, indicating that the reported trends may be influenced by the experimental methods used, the effect of ambient pressure on laminar flame was assumed negligible.

In an investigation (ref. 16) of turbulent Bunsen-type flames, the turbulent flame speed $u_{f,t}$ was correlated by means of the following relation:

$$u_{f,t} = 0.18\, u_f\, Re^{0.24}\, d^{0.26} \tag{16}$$

where d is the tube diameter. If the turbulent flame speed is controlled by the increase in flame surface area resulting from "wrinkling" of the flame, and equation (16) is used to estimate the effects of combustor-inlet Reynolds number on the total flame area A_f, the exponent p in equation (14) would be equal to 0.24. However, there are no data available for the case of the intense mixing conditions existing in turbojet combustors as the result of the impinging air jets and very high Reynolds numbers.

For the normal combustor operating conditions, it was assumed that the effects of both pressure and combustor-inlet Reynolds number on flame speed were minor. Equation (14) then reduces to

$$\eta_b = f\left(\frac{P_i^{1/3}\, T_i^{1.1}}{V_r}\right) \tag{17}$$

if the effect of temperature on the normal flame speed of isooctane (ref. 12) is included. It is noted, however, that if both pressure (ref. 14) and Reynolds number (ref. 16) effects on flame speed are included, the relative exponents of inlet pressure and velocity would be approximately the same as presented in equation (17).

The parameter derived from the assumption that flame spreading governs the over-all combustion rate did not correlate the data for combustor A, as evidenced by the scatter of data points in figure 5. A majority of the data points do, however, lie close to a common curve.

It is therefore indicated that the flame-speed parameter might possibly serve to correlate data over a part of the combustor operating range, and a more critical evaluation of this parameter appears to be warranted.

Other Conversion Processes

In addition to those already discussed, analyses of the turbojet combustion process were also made with the assumption that (1) fuel vaporization, (2) fuel-air turbulent mixing, and (3) fuel-droplet burning (governed by heat transfer into the droplet) were the rate-determining steps in the over-all combustion process. With each of these three analyses, the predicted effects on combustion efficiency of operating variables such as combustor-inlet pressure, combustor velocity, and combustor-inlet temperature, differed markedly from the effects observed experimentally; that is, the equations relating P_i, T_i, and V_r derived in these analyses differed markedly from equation (7) and gave no correlation of experimental data. Reference 17 presents the change in burning rate of single fuel droplets resulting from a change in oxygen concentration of the ambient atmosphere. This change in droplet-burning rate is shown to be much less than that required for this phenomenon to account for the observed change in combustion efficiency with change in inlet oxygen concentration in a typical turbojet combustor.

Since none of these three analyses provided agreement between theoretical and experimental data, the tentative conclusion may be drawn that neither fuel vaporization, fuel-air mixing, nor fuel-droplet burning alone constitutes the rate-determining, slowest step in the combustion process. The analyses were, however, based on certain simplifying assumptions similar to the assumptions included in the analyses of the chemical reaction kinetics and flame spreading, which were previously discussed. Therefore, the possibility cannot be overlooked that difference assumptions in these analyses might result in closer agreement between theory and experimental data.

EXPERIMENTS TO VERIFY THEORY

Variation of Oxygen Concentration

In order to test the applicability of the equations previously derived, a number of special experiments were conducted. Investigations of vapor-fuel - oxygen - nitrogen mixtures have shown marked effects of oxygen concentration on such fundamental combustion properties as minimum spark-ignition energy, quenching distance, and flame speed (refs. 12 and 18). Oxygen concentration appreciably affects equilibrium flame temperature at stoichiometric or richer fuel-air ratios and also affects the concentration of the chemical species involved in the combustion; oxygen concentration is therefore a means of varying the kinetics of the chemical reactions. In combustor tests, variations in oxygen concentrations should affect the rate of combustion without appreciably changing such factors as inlet velocity, turbulent mixing as associated with inlet conditions, and the fuel-spray characteristics. This experimental device should

simplify interpretation and application of the test data. Accordingly, an investigation was conducted to determine the effect of inlet-oxygen concentration on the combustion efficiency of turbojet combustor B. Combustion-efficiency data were obtained for the combustor operating both with liquid isooctane and with gaseous propane over a range of combustor-inlet pressures and oxygen concentrations. The combustor-inlet temperature and the oxygen-nitrogen-mixture mass-flow rate were held constant in all tests.

A typical set of data obtained for the combustor operating with liquid isooctane and gaseous propane is shown in figure 6. There are pronounced changes in combustion efficiency with variation in both combustor-inlet pressure and oxygen concentration. Data of this type were treated in terms of both the second-order reaction and the flame-speed equations previously derived.

In the application of equation (5) to the oxygen-enrichment data, the burning-zone temperature was arbitrarily taken as the stoichiometric adiabatic equilibrium temperature and the concentration of one of the reactants was assumed to be proportional to the oxygen concentration α of the combustor-inlet oxygen-nitrogen mixture. Under these conditions, the ratio N_A/N_B can be assumed constant, and for a given combustor, fuel, and fuel-oxygen-nitrogen mixture ratio, equation (5) can be expressed in the form

$$\eta_b = f\left[\frac{\alpha P_i T_i}{V_r}\left(\frac{e^{-\frac{E}{RT_{eq}}}}{T_{eq}^{3/2}}\right)\right] \tag{18}$$

Here T_{eq} is the stoichiometric adiabatic equilibrium temperature, which is a function of oxygen concentration. The application of equation (18) to the data of figure 6(a) is shown in figure 7. The equilibrium temperatures at the various combustor-inlet pressures and oxygen concentrations were computed by the methods and charts of reference 19. For the combustor data obtained with liquid isooctane, it was found that an apparent energy of activation of approximately 37,000 calories per gram mole satisfactorily correlated the data. This value is in reasonable agreement with the apparent energy of activation of 32,000 calories per gram mole obtained from adiabatic compression data for isooctane-air mixtures (ref. 20). In reference 12, it was found that for flame-speed data of isooctane-oxygen-nitrogen mixtures, a value of 40,000 gave closer agreements between experimental and predicted flame speeds than did 32,000 calories per gram mole. The effect of fuel-air ratio on the form of the correlation curves is shown in figure 8. Here, the faired curves drawn through the correlated data are plotted for the various fuel-flow rates.

The data obtained for the combustor operating with gaseous propane were correlated in a similar fashion. Figure 9 shows the correlation in terms of equation (18) for the combustor operating at a fuel-air ratio of 0.012. The value of apparent energy of activation E required for best correlation varied from approximately 27,000 in the low combustion-efficiency range to approximately 33,000 calories per gram mole in the high combustion-efficiency range. Since the scatter of the correlation in the low combustion-efficiency range was quite sensitive to the value E, figure 9 was obtained using a value of E of 28,000 calories per gram mole. The accuracy of measurements of combustor operating variables was not good enough to warrant the determination of a more exact value of E between 27,000 and 33,000 calories per gram mole. This range of values for E is in approximate agreement with those cited for propane in the literature. In reference 20, a value of 38,000 calories per gram mole is given. This value was used in reference 21 in the application of the Semenov theory to flame-speed data of propane-oxygen-nitrogen mixtures. However, unpublished observations by the authors of reference 21 indicated that a value of 34,000 calories per gram mole resulted in an improvement between experimental and predicted values.

For combustor data obtained at constant inlet temperature and weight-flow rate of the inlet oxygen-nitrogen mixture, the flame-spreading equation (eq. (14)) reduces to

$$\eta_b = f\left(\frac{P_i^{1/3} u_f}{V_r}\right) \tag{19}$$

Here the small change in Reynolds number resulting from the change in viscosity of the inlet mixture with oxygen concentration is neglected.

In reference 12, the laminar flame speeds of isooctane-oxygen-nitrogen mixtures at atmospheric pressure and various equivalence ratios were determined over a range of initial mixture temperatures and oxygen concentrations. The maximum flame speed u_f was found to be directly proportional to the term $(\alpha - 12)$. In reference 21, similar data were obtained for propane-oxygen-nitrogen mixtures. A correlation term similar to that of equation (19) was also obtained. In order to provide a more accurate representation of the flame speeds at the low oxygen concentrations used in the combustor experiments, this type of correlation term was applied to the data of reference 21 for oxygen concentrations of 30 percent by volume and below. For this range of oxygen concentrations, the flame speed was found to be proportional to the term $(\alpha - 11.5)$. It is noted that this value of 11.5, which represents the extrapolated value of α for zero u_f, is in agreement with the value of 11.6 cited in reference 22 for the concentration limit of flammability. Substituting these correlation terms

for the effect of oxygen concentration on maximum flame speed in equation (19) gives the following flame-speed equations for the case of constant combustor-inlet temperature:

For isooctane,

$$\eta_b = f\left[\frac{P_i^{1/3}(\alpha - 12)}{V_r}\right] \tag{20}$$

For propane,

$$\eta_b = f\left[\frac{P_i^{1/3}(\alpha - 11.5)}{V_r}\right] \tag{21}$$

In equations (20) and (21), the laminar flame speeds of both isooctane and propane were assumed independent of pressure. Figures 10 and 11 present a correlation of the combustion-efficiency data for isooctane and propane in terms of the preceding flame-speed parameters. It is seen that the parameters of equations (20) and (21) satisfactorily correlate the combustion-efficiency data.

Independent Variation of Combustor-Inlet Pressure and Air-Flow Rate over Wide Ranges

The assumption that chemical reaction kinetics govern the over-all combustion rates led to the prediction that combustion efficiency could be correlated as a function of the parameter $\frac{P_i T_i}{V_r}$, and this parameter is equal to a dimensional constant times the parameter $\frac{P_i^2}{W_a}$. The assumption that the rate of flame spreading governs the over-all combustion rate led to the prediction that combustion efficiency should correlate as a function of the parameter $\frac{P_i^{1/3} T_i^{1.1}}{V_r}$. This parameter is equivalent to a dimensional constant times $\frac{P_i^{1.3} T_i^{0.1}}{W_a}$. The reaction kinetics analysis therefore yields a ratio of exponents of the pressure and air-flow rate

terms of 2, while the flame-speed analysis yields a ratio of these same exponents of 1.3. Obviously both of these parameters cannot adequately correlate the combustion-efficiency data where the combustor pressure and combustor air-flow rate are varied through wide ranges. Both of these parameters did, however, provide a satisfactory correlation of the data for combustor B (figs. 7, 9, 10, and 11) because these data were obtained for combustor operation at a single value of air-flow rate. The correlations of the data for combustor A (figs. 4 and 5) indicated that $\frac{P_i T_i}{V_r}$ better correlated these data than did the flame-spreading parameter $\frac{P_i^{1/3} T_i^{1.1}}{V_r}$; the flame-spreading parameter served to correlate at least the majority of the data points, however. The data for combustor A were obtained at simulated engine operating conditions and therefore did not include very large independent variations of P_i and W_a.

In order to determine conclusively whether the ratio of exponents on the pressure and air-flow rate terms should be 2 or 1.3, it was therefore necessary to conduct a series of combustor tests in which the pressure and air-flow rate were independently varied over wide ranges of operating conditions. Such an investigation was conducted in turbojet combustor B, using gaseous propane fuel and a single-orifice fuel injector. A sample of the experimental data is shown in figure 12, where combustion efficiency is plotted against combustor-inlet pressure with parametric lines of air-flow rate. The data of figure 12 are for a fuel-air ratio of 0.012; similar data were obtained for fuel-air ratios of 0.008 and 0.016.

Figure 13(a) shows a cross plot of the data of figure 12; combustor air-flow rate is plotted against combustor pressure with parametric lines of combustion efficiency. The slope of the lines in figure 13(a) indicates the ratio of exponents on the pressure and air-flow rate terms of the correlating parameter which best fits the experimental data. A transition is evident in the vicinity of a combustor pressure of 15 inches of mercury. At the very low values of combustor pressure and air-flow rate, the slope of the curves is approximately 2, which agrees with the slope predicted by the parameter $\frac{P_i T_i}{V_r}$. At high values of combustor air-flow rate and pressure, however, the slope of the curves is of the order of 1.3, which agrees with the value predicted by the parameter $\frac{P_i^{1/3} T_i^{1.1}}{V_r}$.

Similar plots of the data obtained at fuel-air ratios of 0.008 and 0.016 are shown in figures 13(b) and 13(c), respectively. The data of figure 13(b) again indicate a transition in the curves, with the slope being approximately 2 at low values of pressure and air-flow rate and approximately 1.3 at the higher values of pressure and air-flow rate. The data for a fuel-air ratio of 0.016 do not extend to pressures below about 14 inches of mercury; hence the transition in slope of the curves was not obtained in figure 13(c).

The data of figure 13 indicate that for this particular combustor, the parameter $\frac{P_i T_i}{V_r}$ will correlate data obtained at the low values of pressure and air-flow rate, while the parameter $\frac{P_i^{1/3} T_i^{1.1}}{V_r}$ will correlate the data obtained at higher values of pressure and air-flow rate. Neither parameter, however, adequately correlates data obtained over the entire range of pressures and air-flow rates. This prediction is verified by the data of figures 14 and 15, where the data of figure 12 are plotted as a function of the parameters $\frac{P_i T_i}{V_r}$ and $\frac{P_i^{1/3} T_i^{1.1}}{V_r}$, respectively.

Although the data of figure 13 are meager and therefore insufficient to warrant conclusions regarding the combustion mechanism, there is some indication that a shift from one rate-controlling process to some other rate-controlling process occurs as combustor operating conditions are varied through wide ranges. The data of figure 13, together with the analyses presented earlier in this paper, indicate that at very low values of pressure in the combustor, the chemical reaction kinetics is the rate-controlling process. At higher pressures, however, the rate of flame spreading would appear to be the rate-determining process. This trend of events is at least in qualitative accord with expectations, for the chemical reaction kinetics are a function of the square of combustor pressure and would therefore be expected to be very slow at low-pressure conditions and increase rapidly with increase in pressure until some pressure is reached above which kinetics no longer constitute the slowest step in the over-all chain of processes. More extensive investigations with other combustors are required, however, before any definite conclusions could be made in this regard.

References 4 and 5 show combustion efficiency of a small-scale ram-jet combustor to be correlated by a flame-spreading equation that is quite similar to equation (17). This ram-jet combustor would not operate at very low pressures; hence, the performance of this combustor followed the same general trends as turbojet combustor B at comparable pressures. This

is in accordance with expectations, since there is no apparent fundamental difference between the combustion process in ram-jet and turbojet combustors.

CONCLUDING REMARKS

The parameter $\frac{P_i T_i}{V_r}$ (P_i is combustor-inlet static pressure, T_i is combustor-inlet static temperature, and V_r is combustor reference velocity based on P_i, T_i, and maximum combustor cross-sectional area), which was derived from the assumption that chemical reaction kinetics controls combustor performance, provided an adequate correlation of the combustion-efficiency data of one turbojet combustor at simulated engine operating conditions. These same data were not correlated by the parameter $\frac{P_i^{1/3} T_i^{1.1}}{V_r}$, derived from the assumption that the rate of flame spreading controls combustor performance. Data obtained with another turbojet combustor indicated that a shift from one rate-controlling step to another occurred as combustor pressure was increased, and the parameter $\frac{P_i T_i}{V_r}$ therefore best correlated the data at low pressures while the parameter $\frac{P_i^{1/3} T_i^{1.1}}{V_r}$ was better at higher pressures. No single correlating parameter can therefore be expected to be adequate for all combustors and for the entire range of operating conditions.

Because of the complexity of the over-all process of turbine-engine combustion, it would appear unlikely that this simplified theoretical treatment (which assumes one step in the chain of conversion processes to be rate-controlling) would be adequate for all combustors. Previous investigations have shown that the parameter $\frac{P_i T_i}{V_r}$ is not adequate for correlating the data for certain turbojet combustors, even for the limited range of conditions required to simulate flight operation. In addition, experimental data are available that indicate fuel vaporization and fuel-air mixing play an important role in some combustors (for example, ref. 23). Consequently, the equations derived in this paper must be applied judiciously and with due regard for their limitations.

Lewis Flight Propulsion Laboratory
National Advisory Committee for Aeronautics
Cleveland, Ohio, July 21, 1954

APPENDIX - SYMBOLS

The following symbols were used in this report:

$A_{H,P}$	liner open-hole area in combustor reaction zone, sq ft
$A_{H,T}$	total liner open-hole area, sq ft
A_a	average cross-sectional area of combustor reaction zone, sq ft
A_f	total flame-surface area in combustor, sq ft
A_r	maximum cross-sectional area of combustor flow passage, sq ft
a_f	flame surface-area per unit volume, ft^{-1}
d	tube diameter
E	energy of activation for reaction, ft-lb/lb
f	over-all fuel-oxygen-nitrogen-mixture ratio
K_1, K_2, K_3, etc.	constants
L	length of reaction zone, ft
l	distance from upstream end of reaction zone to plane of any point within reaction zone, ft
N_A, N_B	number of molecules of reactant A and B per pound original mixture, lb^{-1}
P	static pressure in combustor reaction zone, lb/sq ft abs
ΔP	static pressure drop across combustor, lb/sq ft abs
P_i	combustor-inlet static pressure, lb/sq ft abs
R	gas constant, ft-lb/lb $^{\circ}R$
Re	Reynolds number

T	absolute static temperature in combustor reaction zone, $^{\circ}R$
T_{eq}	equilibrium flame temperature, $^{\circ}R$
T_i	combustor-inlet absolute static temperature, $^{\circ}R$
ΔT_s	temperature rise for complete combustion of stoichiometric mixture, $^{\circ}F$
u_f	laminar flame speed, ft/sec
$u_{f,t}$	turbulent flame speed, ft/sec
V_a	velocity based on density, mass flow, and average cross-sectional area of reaction zone, ft/sec
V_r	reference velocity based on combustor-inlet density, total air flow, and maximum cross-sectional area of combustor flow passage, ft/sec
W_a	combustor air-flow rate, lb/sec
$\frac{dw}{d\theta}$	reaction rate, lb mixture reacting/(sec)(cu ft)
X	fraction of N reacted at any time θ or at any location within reaction zone
Z	number of molecular collisions of type involved in reaction, per unit volume per unit time, ft^{-3} sec^{-1}
α	volume percent oxygen concentration at combustor inlet
β	probability factor, fraction of collisions involving sufficient energy for reaction to occur which actually result in reaction
η_b	combustion efficiency
θ	time, sec
ρ	density, lb/cu ft
σ_A, σ_B	effective molecular diameter of reactants A and B, ft
φ	fraction of collisions involving sufficient energy for reaction to occur

REFERENCES

1. Childs, J. Howard: Preliminary Correlation of Efficiency of Aircraft Gas-Turbine Combustors for Different Operating Conditions. NACA RM E50F15, 1950.

2. Graves, Charles C.: Effect of Oxygen Concentration of the Inlet Oxygen-Nitrogen Mixture on the Combustion Efficiency of a Single J33 Turbojet Combustor. NACA RM E52F13, 1952.

3. Graves, Charles C.: Effect of Inlet Oxygen Concentration on Combustion Efficiency of J33 Single Combustor Operating with Gaseous Propane. NACA RM E53A27, 1953.

4. Reynolds, Thaine W., and Ingebo, Robert D.: Combustion Efficiency of Homogeneous Fuel-Air Mixtures in a 5-Inch Ram-Jet Type Combustor. NACA RM E52I23, 1952.

5. Reynolds, Thaine W.: Effect of Fuels on Combustion Efficiency of 5-Inch Ram-Jet-Type Combustor. NACA RM E53C20, 1953.

6. Hibbard, Robert R., Drell, Isadore L., Metzler, Allen J., and Spakowski, Adolph E.: Combustion Efficiencies in Hydrocarbon-Air Systems at Reduced Pressures. NACA RM E50G14, 1950.

7. Kassel, Louis S.: The Kinetics of Homogeneous Gas Reactions. Chem. Catalog Co. (New York), 1932.

8. Sobolewski, Adam E., Miller, Robert R., and McAulay, John E.: Altitude Performance Investigation of Two Single-Annular Type Combustors and the Prototype J40-WE-8 Turbojet Engine Combustor with Various Combustor-Inlet Air Pressure Profiles. NACA RM E52J07, 1953.

9. Avery, W. H., and Hart, R. W.: Combustor Performance with Instantaneous Mixing. Ind. and Eng. Chem., vol. 45, no. 8, Aug. 1953, pp. 1634-1637.

10. Longwell, John P., Frost, Edward E., and Weiss, Malcom A.: Flame Stability in Bluff Body Recirculation Zones. Ind. and Eng. Chem., vol. 45, no. 8, Aug. 1953, pp. 1629-1633.

11. Wohlenberg, W. J.: The Influence of Reaction Interface Extension in the Combustion of Gaseous Fuel Constituents. Trans. A.S.M.E., vol. 70, no. 3, Apr. 1948, pp. 143-156; discussion, pp. 156-160.

12. Dugger, Gordon L., and Graab, Dorothy D.: Flame Speeds of 2,2,4-Trimethylpentane-Oxygen-Nitrogen Mixtures. NACA TN 2680, 1952.

13. Gaydon, A. G., and Wolfhard, H. G.: The Influence of Diffusion on Flame Propagation. Proc. Roy. Soc., vol. 196, 1949, pp. 105-113.

14. Garner, F. H., Ashforth, G. K., and Long, R.: The Effect of Pressure on Burning Velocities of Benzene-Air, n-Heptane-Air and 2,2,4-Trimethylpentane-Air Mixtures. Fuel, vol. 30, no. 1, Jan. 1951, pp. 17-19.

15. Hawthorne, W. R., and Fabri, J., eds.: Selected Combustion Problems - Fundamentals and Aeronautical Applications. Butterworths Scientific Pub. (London), 1954, p. 177.

16. Bollinger, Lowell M., and Williams, David T.: Effect of Reynolds Number in the Turbulent-Flow Range on Flame Speed of Bunsen-Burner Flames. NACA Rep. 932, 1949. (Supersedes NACA TN 1707.)

17. Graves, C. C.: Combustion of Single Isooctane Drops in Various Quiescent Oxygen-Nitrogen Atmospheres. Reprint from Proc. Third Midwestern Conf. on Fluid Mech., Univ. of Minn., 1953, pp. 759-778.

18. Lewis, Bernard, and von Elbe, Guenther: Combustion, Flames and Explosions of Gases. Academic Press, Inc. (New York), 1951.

19. Hottel, H. C., Williams, G. C., and Satterfield, C. N.: Thermodynamic Charts for Combustion Processes, Pts. I and II. John Wiley & Sons, Inc. (New York), 1949.

20. Jost, Wilhelm: Explosion and Combustion Processes in Gases. McGraw-Hill Book Co., Inc. (New York and London), 1946, p. 476.

21. Dugger, Gordon L., and Graab, Dorothy D.: Flame Velocities of Propane- and Ethylene-Oxygen-Nitrogen Mixtures. NACA RM E52J24, 1953.

22. Coward, H. F., and Jones, G. W.: Limits of Flammability of Gases and Vapors. Bull. 503, Bur. Mines, 1952.

23. McCafferty, Richard J.: Liquid-Fuel-Distribution and Fuel-State Effects on Combustion Performance of a Single Tubular Combustor. NACA RM E51B21, 1951.

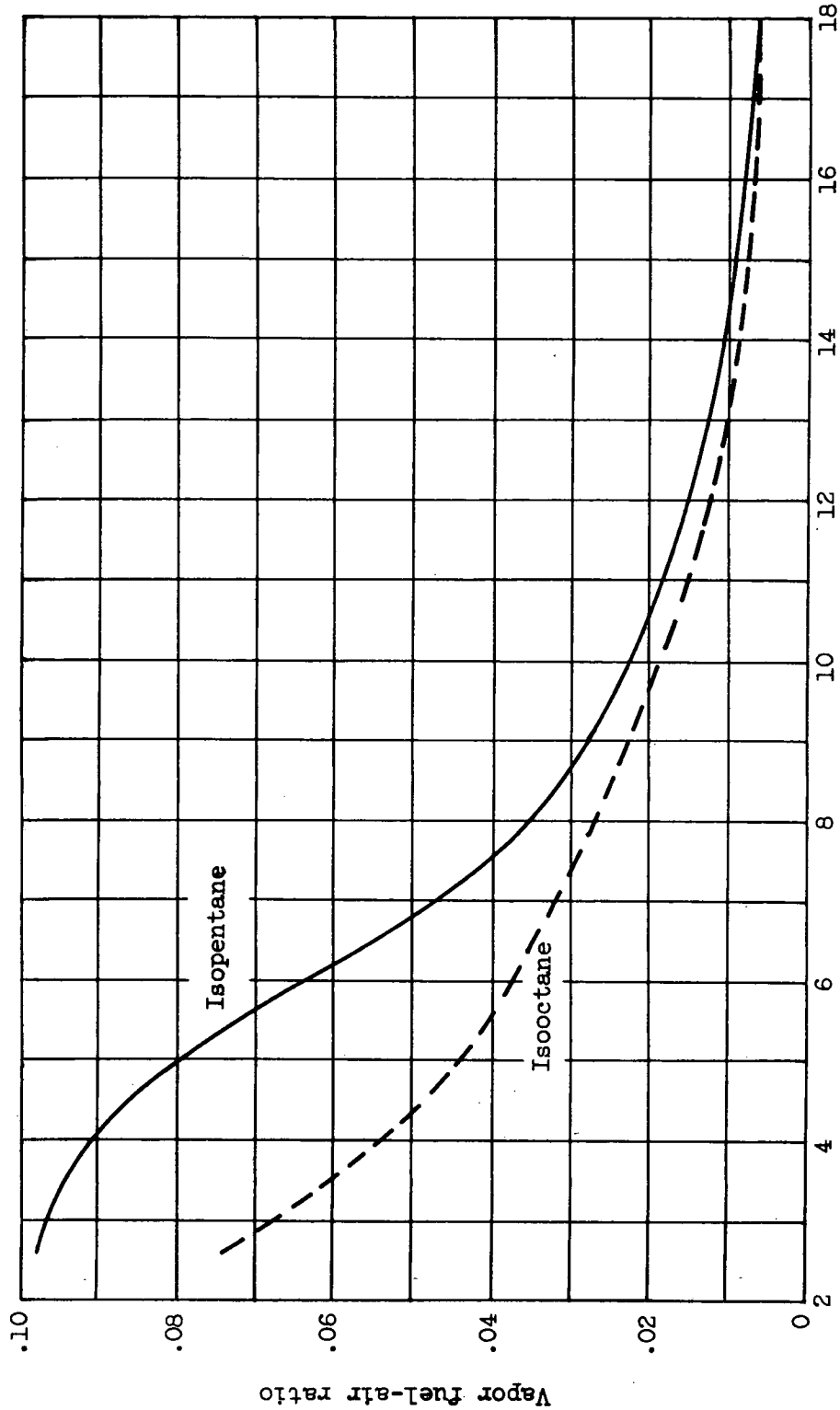

Figure 1. - Variation of vapor fuel-air ratio with distance from fuel nozzle in typical tubular turbojet combustor. Simulated high altitude; over-all fuel-air ratio, 0.007.

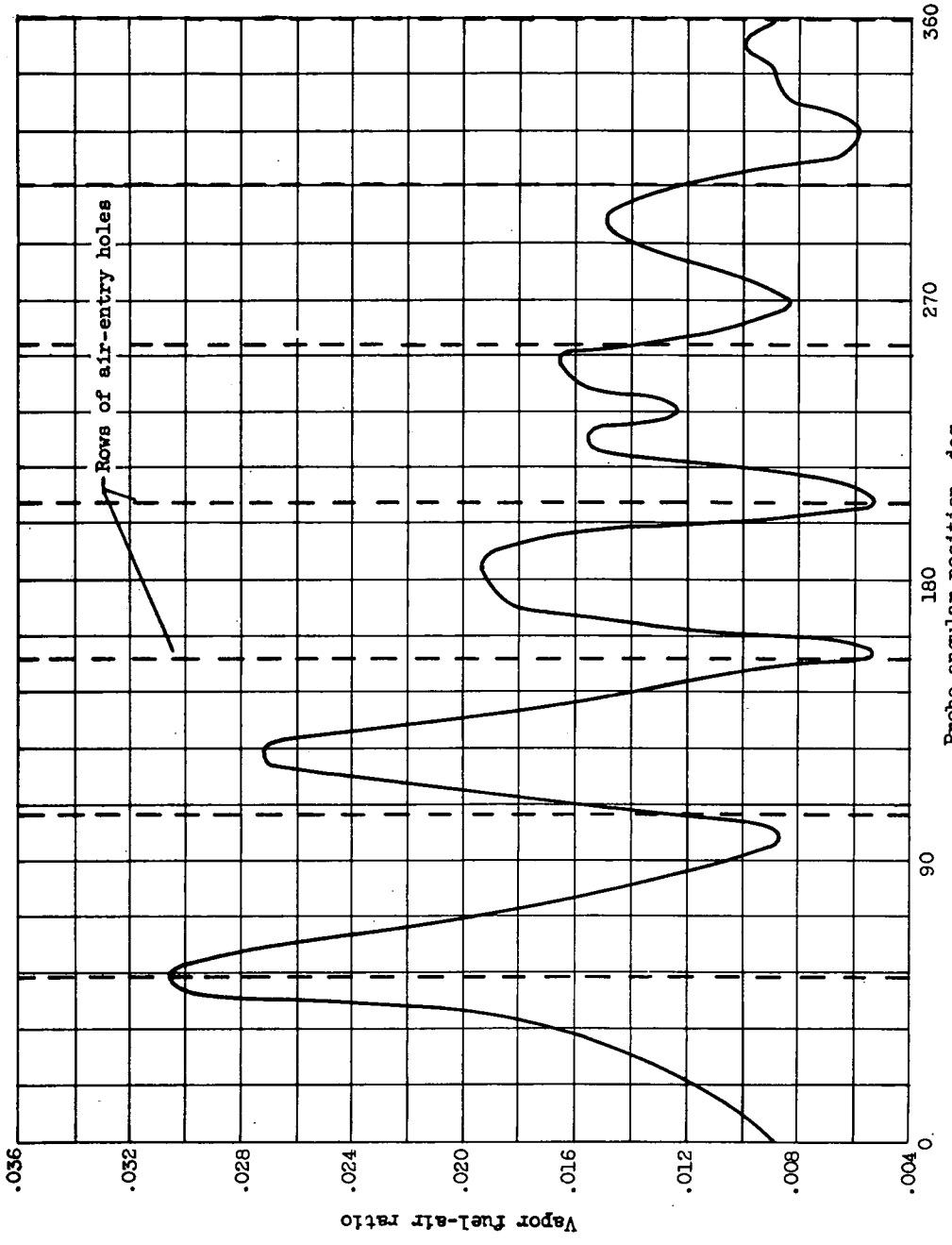

Figure 2. - Variation of fuel-air ratio with angular position of sampling probe $12\frac{1}{2}$ inches downstream of fuel nozzle in a typical tubular turbojet combustor. Fuel, isooctane; over-all fuel-air ratio, 0.014.

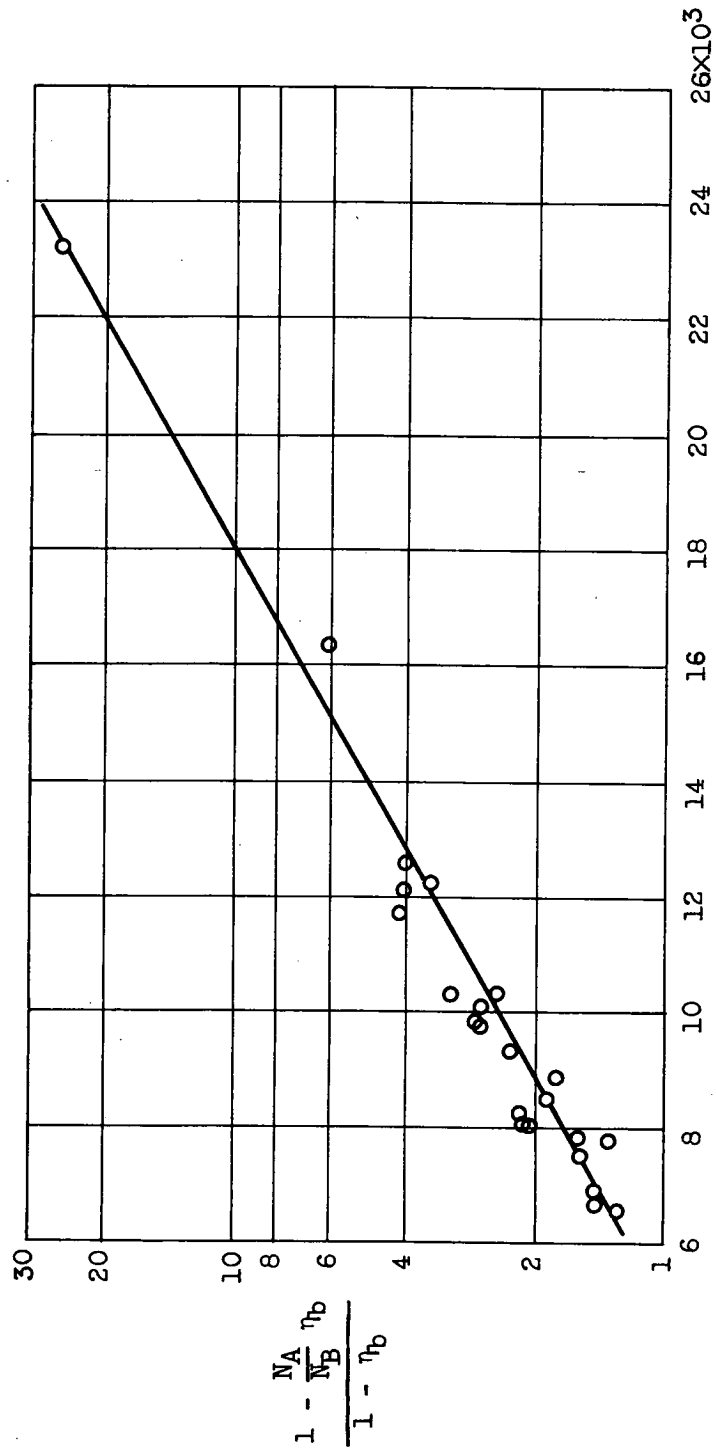

Figure 3. - Experimental data obtained with combustor A plotted in accordance with equation (6). Fuel, gasoline; variable fuel-air ratio.

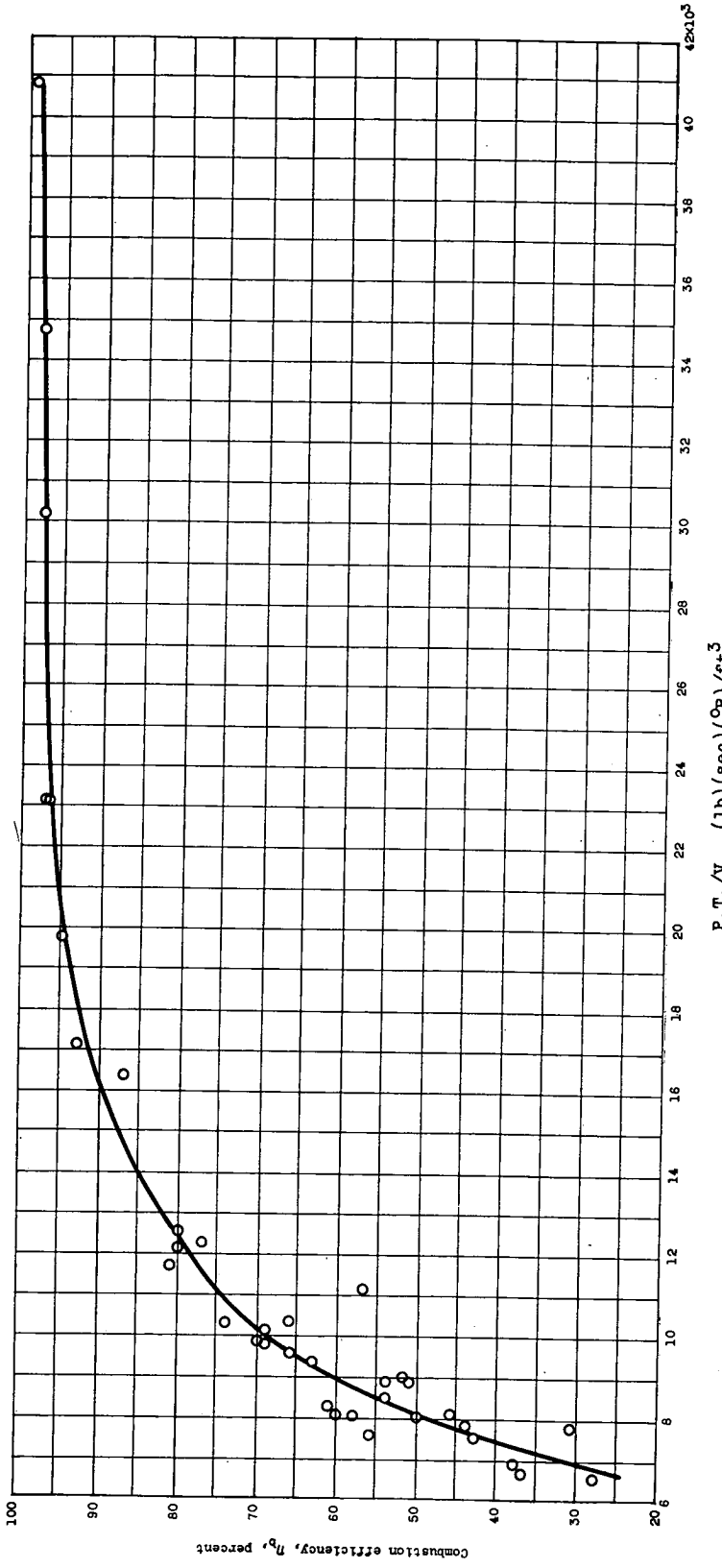

Figure 4. - Experimental data obtained with combustor A plotted in accordance with equation (7). Fuel, gasoline; variable fuel-air ratio.

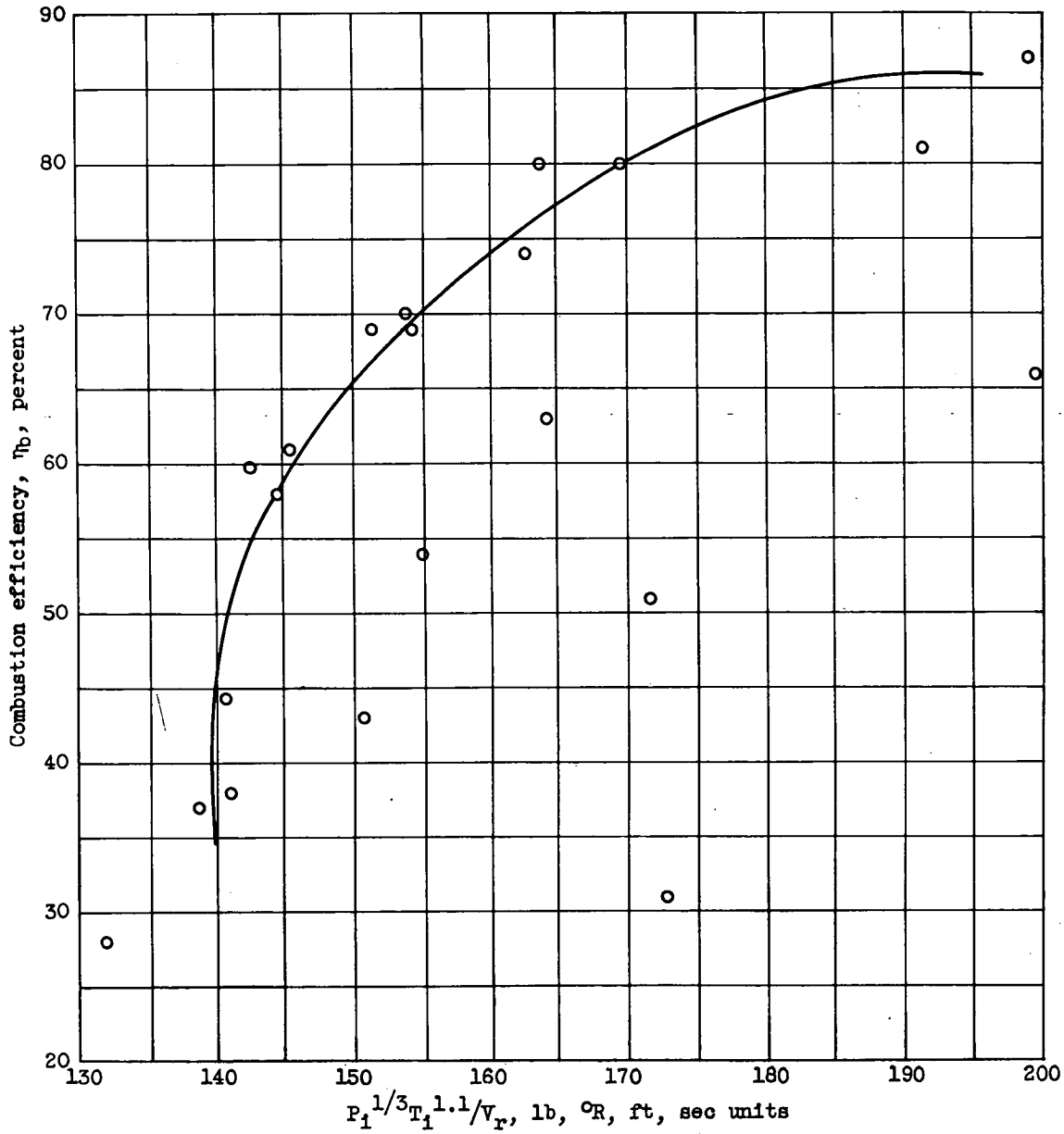

Figure 5. - Experimental data obtained with combustor A plotted in accordance with equation (17). Fuel, gasoline; variable fuel-air ratio.

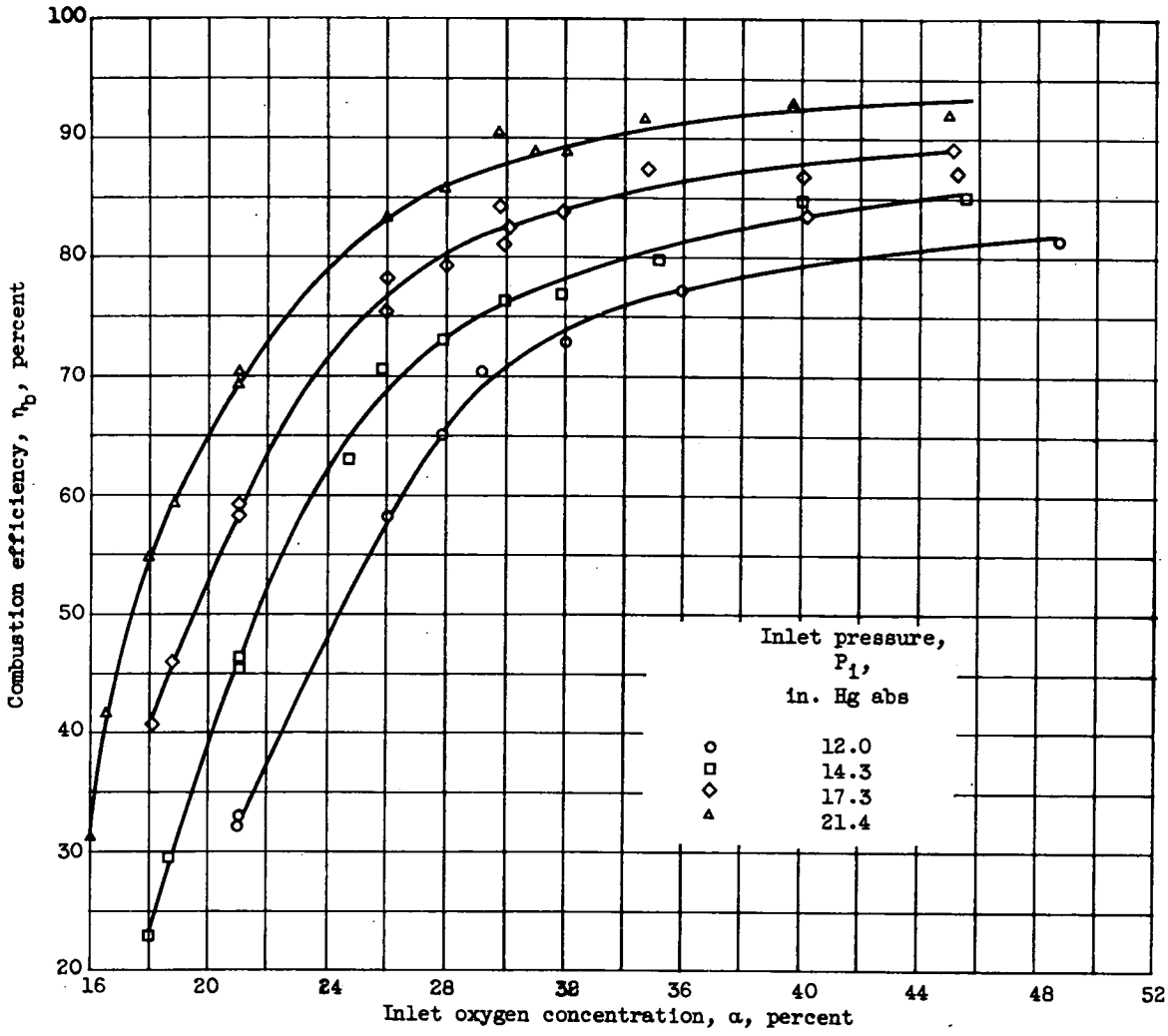

(a) Isooctane fuel.

Figure 6. - Sample of experimental data obtained with combustor B and varying inlet oxygen concentration. Fuel-air ratio, 0.012; inlet temperature, 40° F.

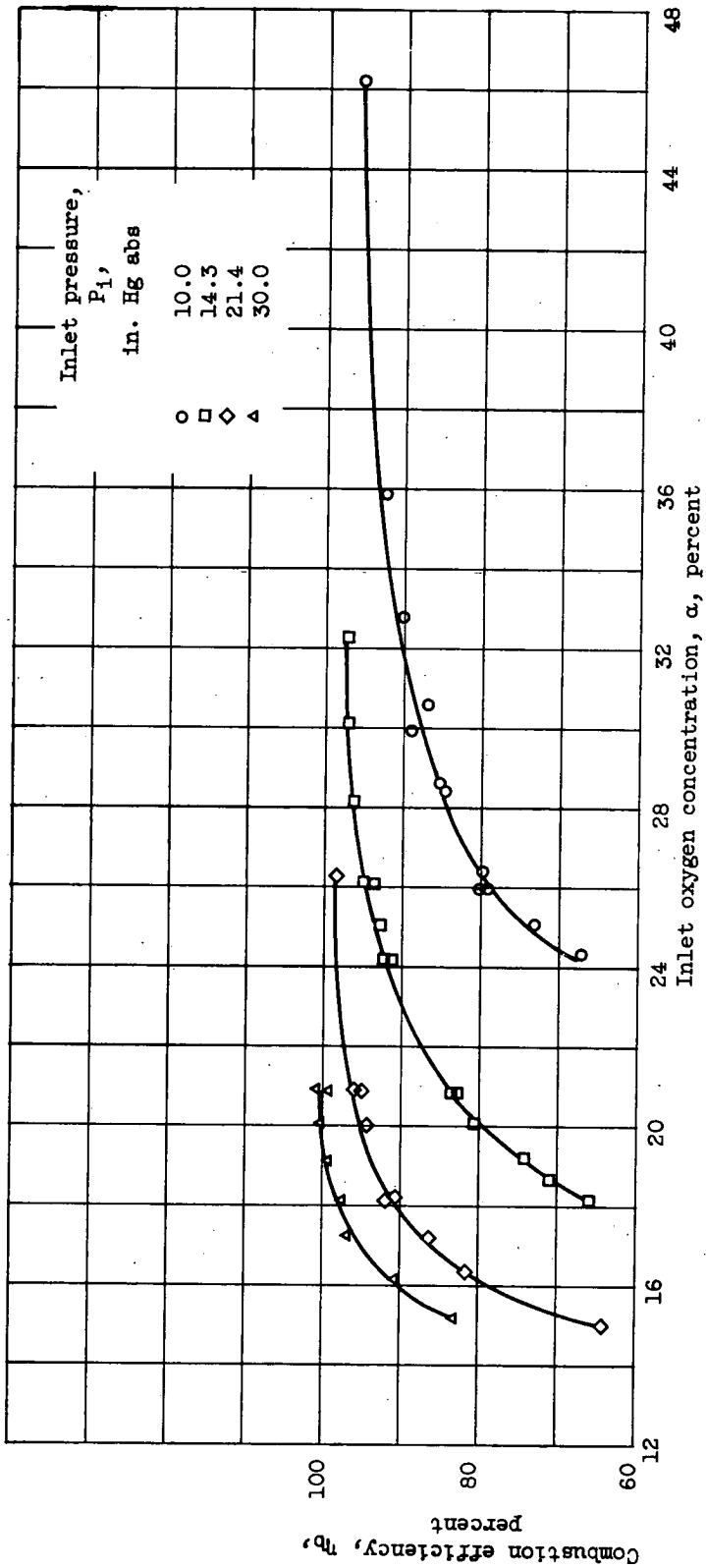

(b) Propane fuel.

Figure 6. - Concluded. Sample of experimental data obtained with combustor B and varying inlet oxygen concentration. Fuel-air ratio, 0.012; inlet temperature, 40° F.

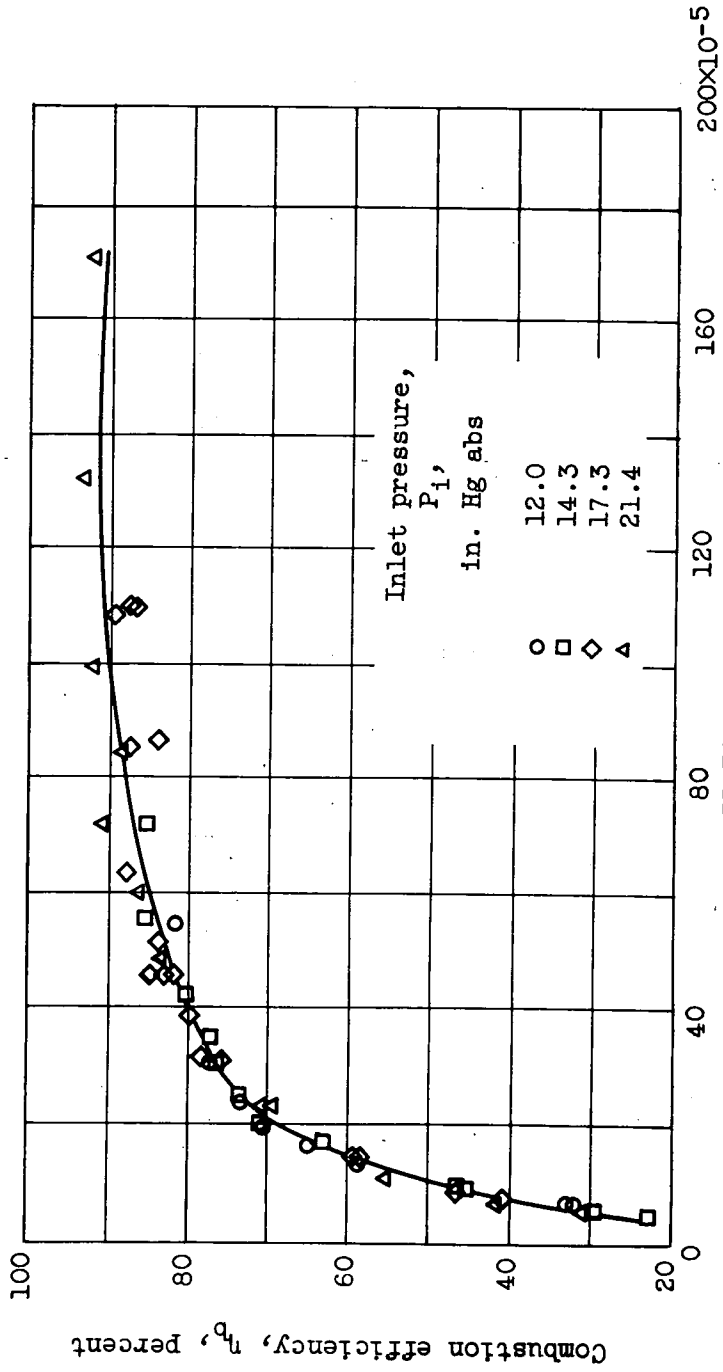

Figure 7. - Experimental data obtained with combustor B (fig. 6(a)) plotted in accordance with equation (18). Fuel, isooctane; fuel-air ratio, 0.012; inlet temperature, 40° F.

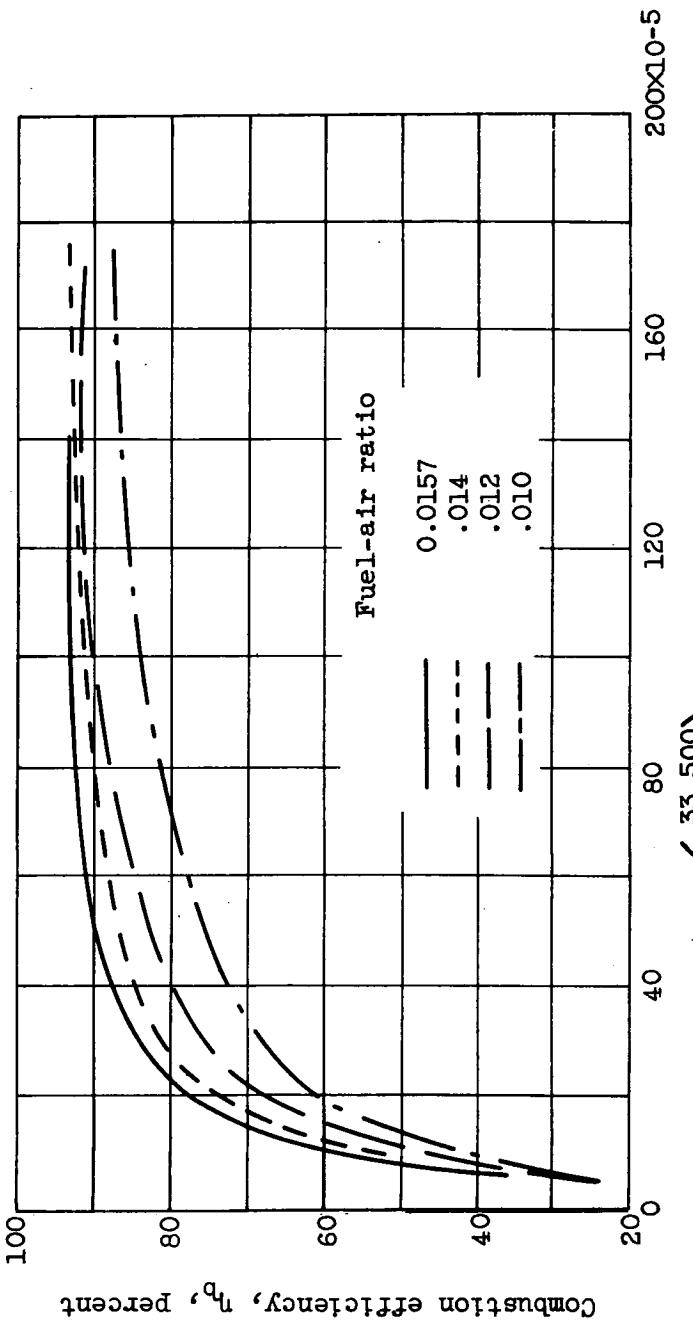

Figure 8. - Effect of fuel-air ratio on correlation of data for combustor B. Fuel, isooctane; inlet temperature, 40° F.

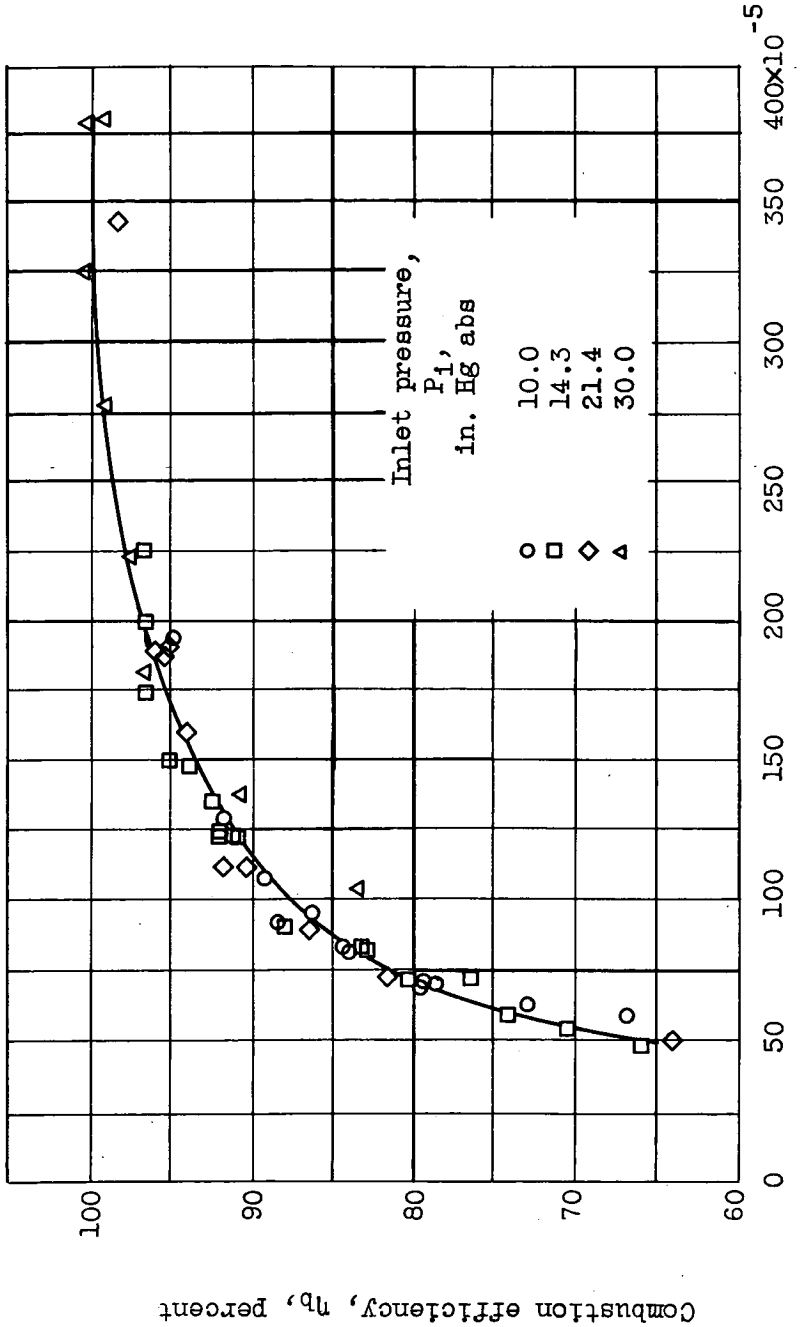

Figure 9. - Experimental data obtained with combustor B (fig. 6(b)) plotted in accordance with equation (18). Fuel, propane; fuel-air ratio, 0.012; inlet temperature, 40° F.

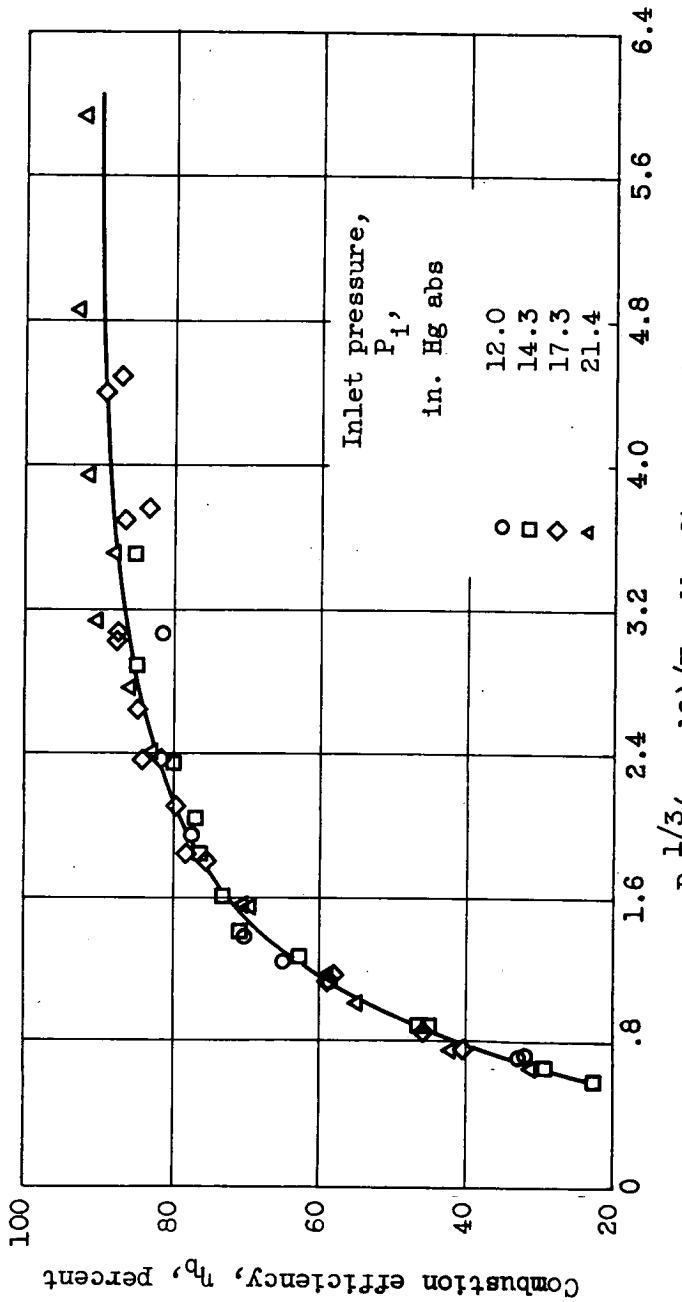

Figure 10. - Experimental data obtained with combustor B (fig. 6(a)) plotted in accordance with equation (20). Fuel, isooctane; fuel-air ratio, 0.012; inlet temperature, 40° F.

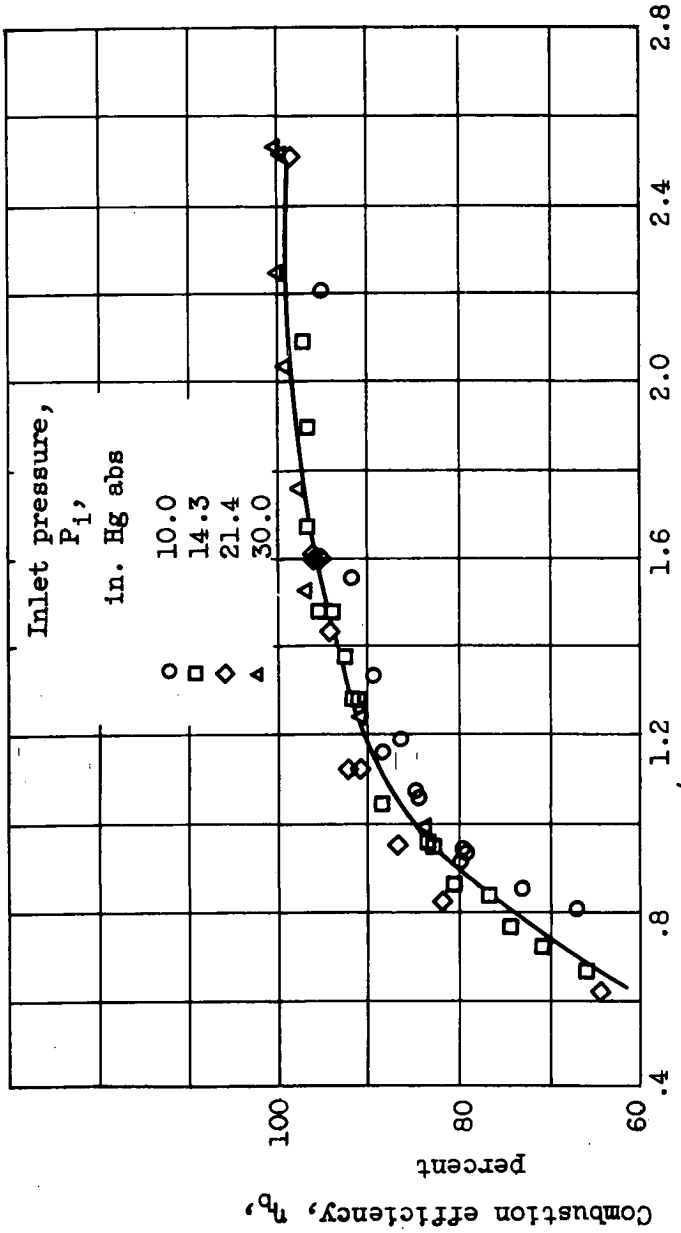

Figure 11. - Experimental data obtained with combustor B (fig. 6(b)) plotted in accordance with equation (21). Fuel, propane; fuel-air ratio, 0.012; inlet temperature, 40° F.

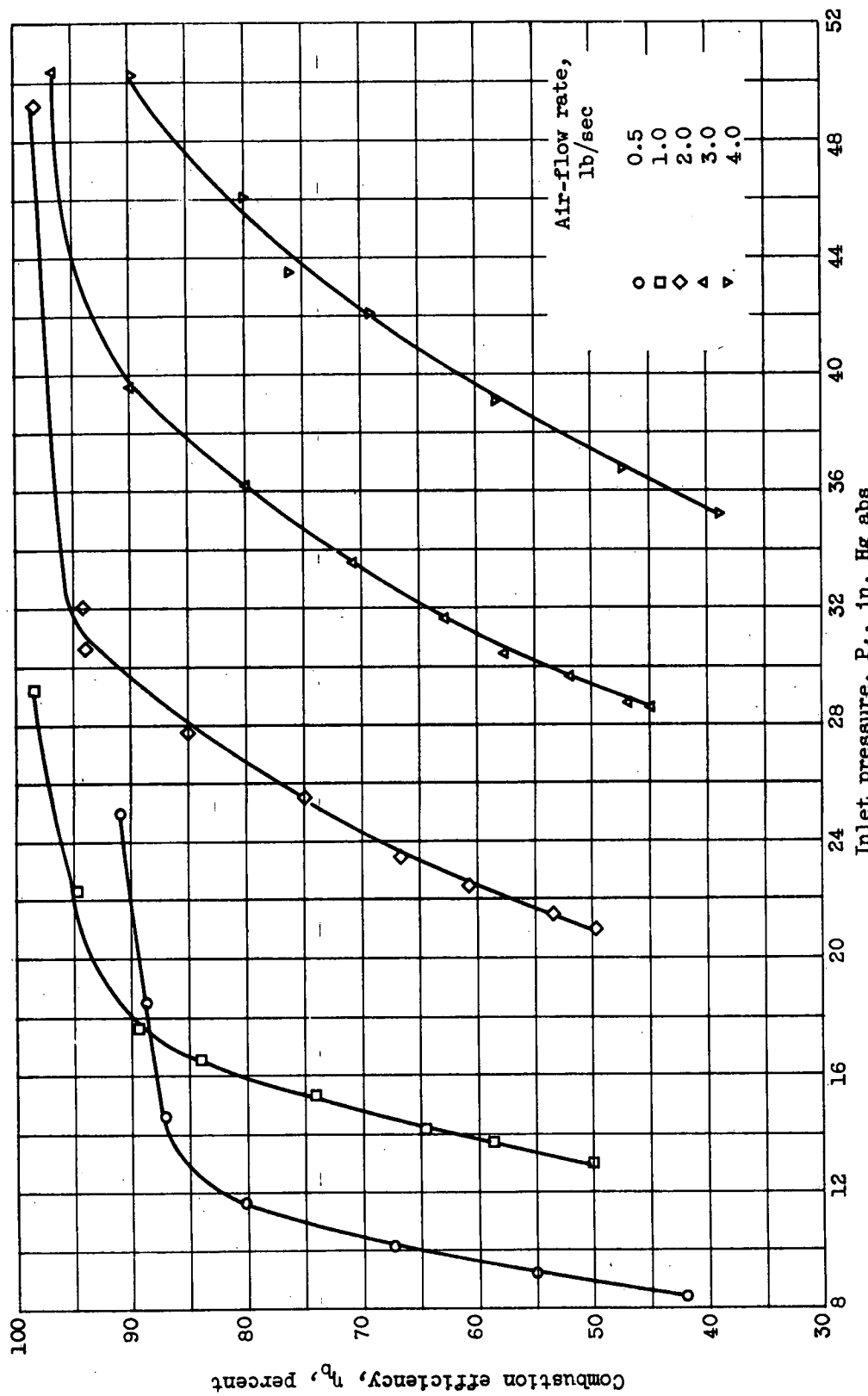

Figure 12. - Sample of data obtained with combustor B for wide variation in inlet pressure and air-flow rate. Fuel, propane; fuel-air ratio, 0.012; inlet temperature, 80° F.

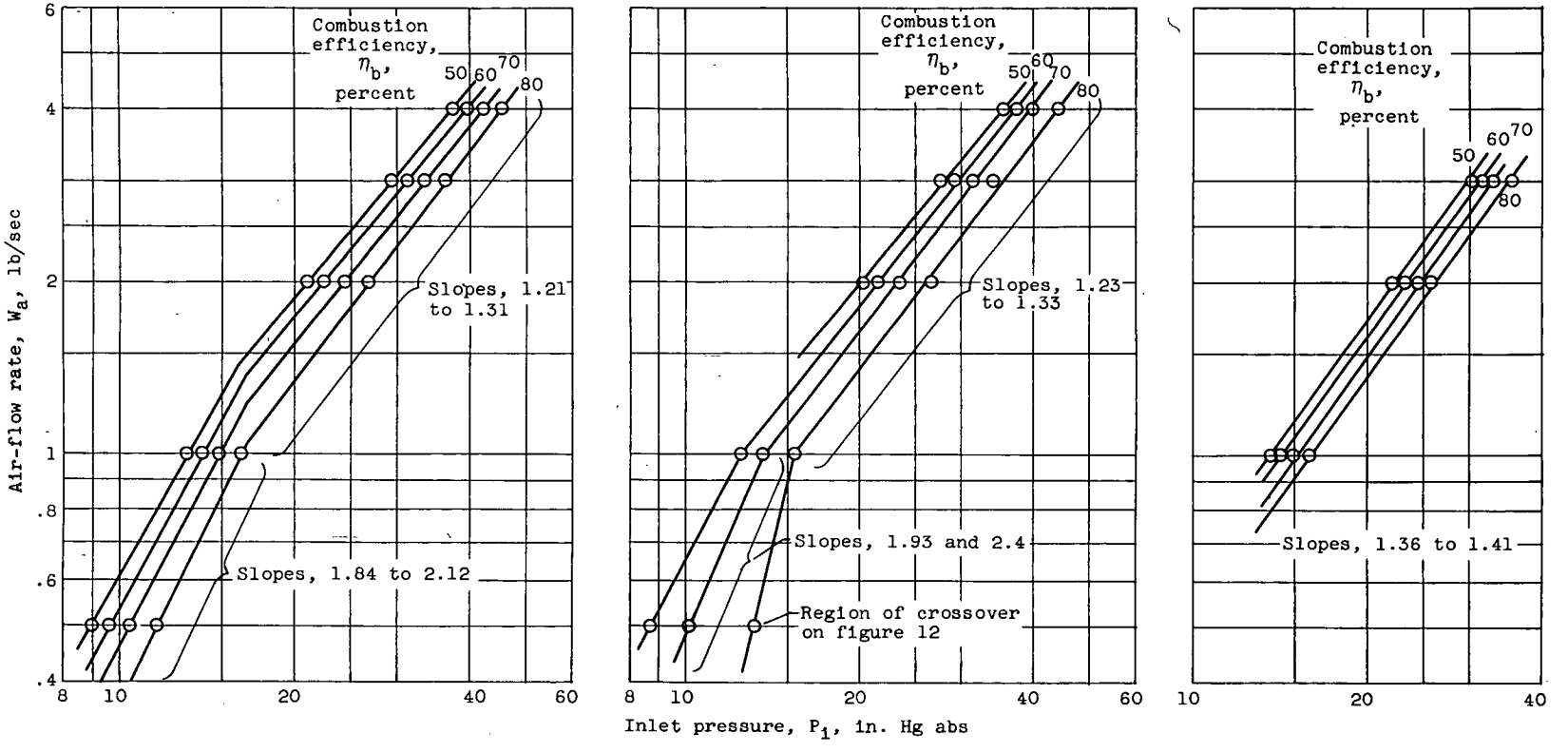

(a) Fuel-air ratio, 0.012.

(b) Fuel-air ratio, 0.008.

(c) Fuel-air ratio, 0.016.

Figure 13. - Cross plot from faired curves of figure 12 to determine relative effects of inlet pressure and air-flow rate on combustion efficiency.

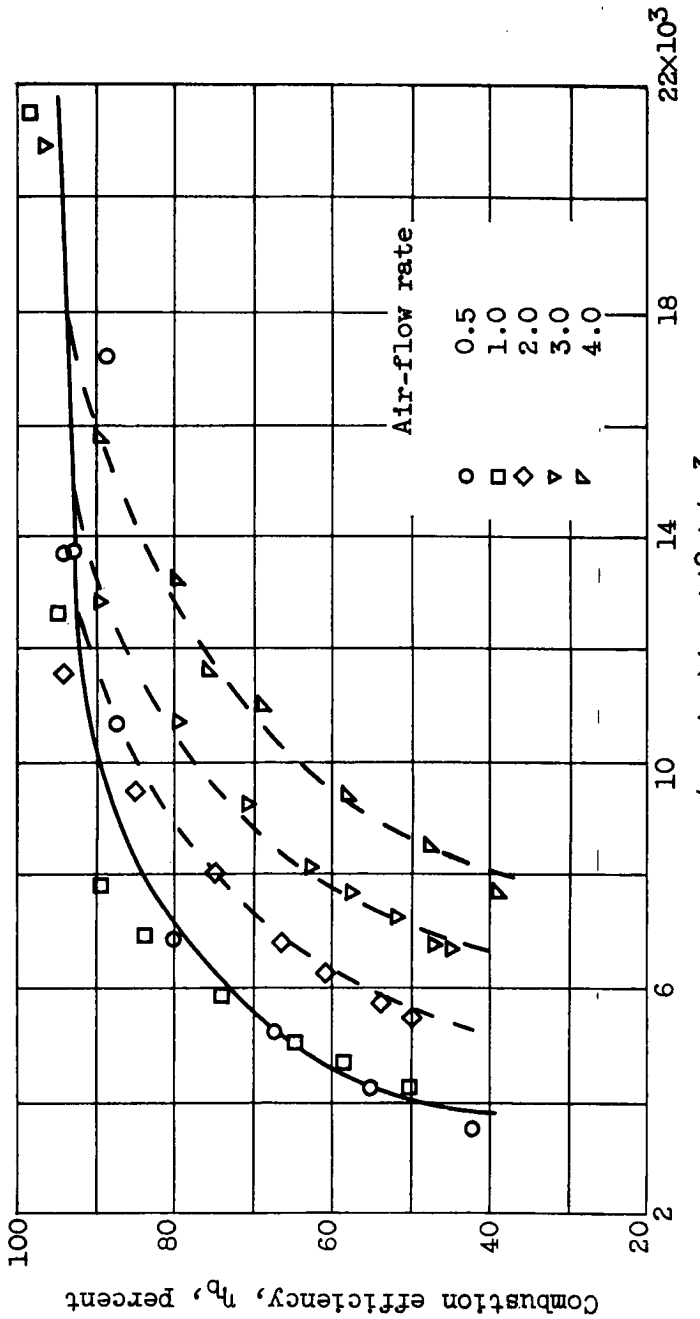

Figure 14. - Experimental data obtained with combustor B (fig. 12) plotted in accordance with equation (7). Fuel, propane; fuel-air ratio, 0.012; inlet temperature, 80° F.

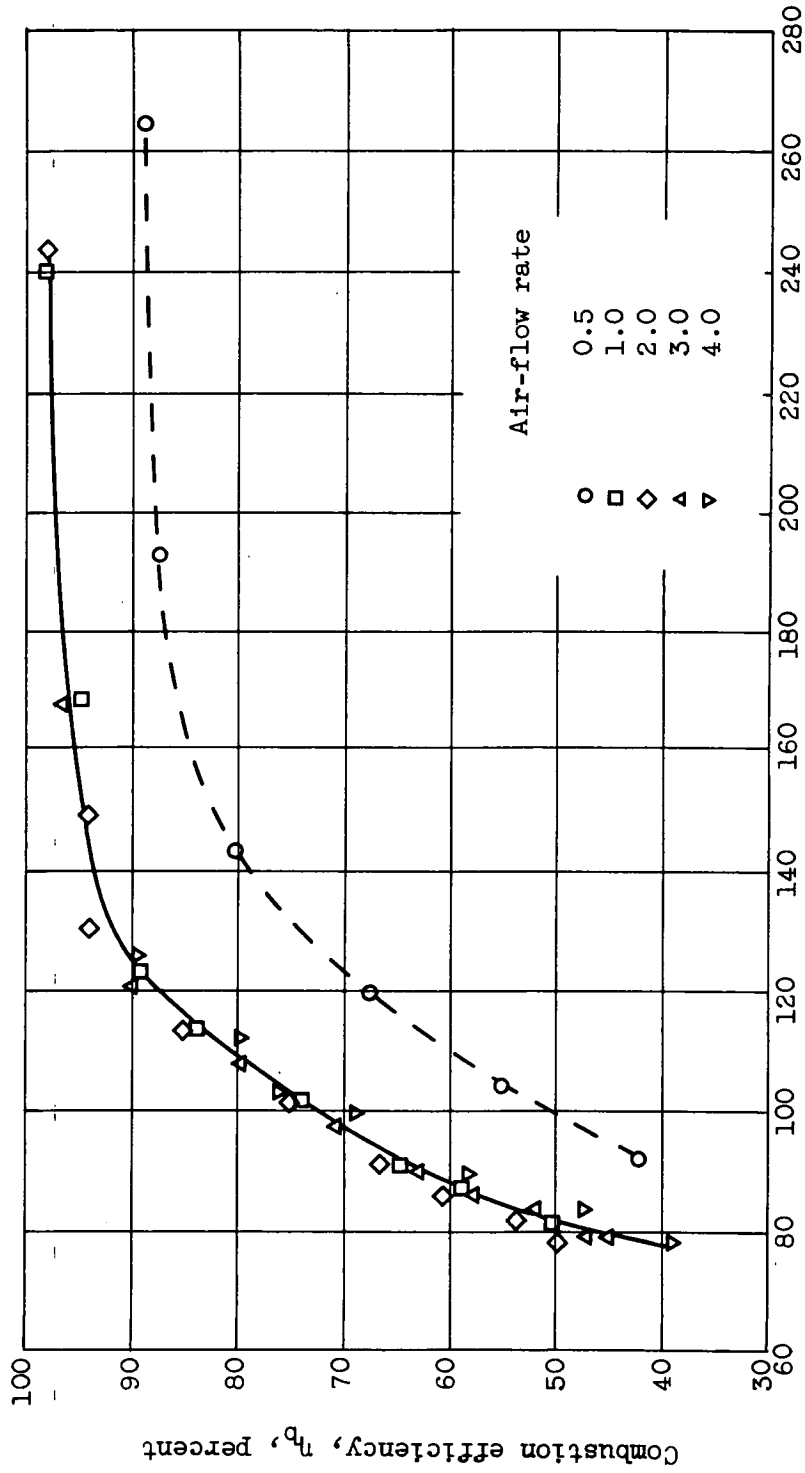

Figure 15. - Experimental data obtained with combustor B (fig. 12) plotted in accordance with equation (17). Fuel, propane; fuel-air ratio, 0.012; inlet temperature, 80° F.